Aerosol and Air Quality Research

ORIGINAL RESEARCH
https://doi.org/10.4209/aaqr.220128

Measurement of Black Carbon in Delhi: Evidences of Regional Transport, Meteorology and Local Sources for Pollution Episodes

Arpit Malik[1,2], Shankar G. Aggarwal[1,2*], Sho Ohata[3,4], Tatsuhiro Mori[5,6], Yutaka Kondo[7], Puna Ram Sinha[8], Prashant Patel[1,2], Baban Kumar[1,2], Khem Singh[1], Daya Soni[1,2], Makoto Koike[6]

[1] CSIR-National Physical Laboratory, New Delhi, India
[2] Academy of Scientific and Innovative Research (AcSIR), Ghaziabad, India
[3] Institute for Space-Earth Environmental Research, Nagoya University, Nagoya, Japan
[4] Institute for Advanced Research, Nagoya University, Nagoya, Japan
[5] Department of Applied Chemistry, Faculty of Science and Technology, Keio University, Yokohama, Japan
[6] Department of Earth and Planetary Science, Graduate School of Science, The University of Tokyo, Tokyo, Japan
[7] National Institute of Polar Research, Tokyo, Japan
[8] Department of Earth and Space Sciences, Indian Institute of Space Science and Technology, Thiruvananthapuram, India

ABSTRACT

Measurement of particulate matter (PM) constituent such as black carbon (BC) over urban sites is critically important owing to its adverse health and climate impacts. However, the impacts associated with BC are poorly understood primarily because of the scarcity and uncertainties of measurements of BC. Here, we present BC measurement at an urban site of Delhi using a characterized continuous soot monitoring system (COSMOS) for a year-long period, i.e., from September, 2019 to August, 2020. This measurement period covers events, i.e., period of crop residue burnings from nearby states, festive events, e.g., Diwali and New Year, and first COVID-19 lockdown period. Effects of these events combining with local emissions and meteorological conditions on BC mass concentration (M_{BC}) are investigated to find the possible cause of severe pollution levels in Delhi. Mean M_{BC} for the complete observation period was found to be 5.02 ± 4.40 μg m^{-3}. M_{BC} showed significant seasonal as well diurnal variations. Winter season (December to February) is observed to be the most polluted season owing to increased local emissions and non-favorable meteorological conditions. Regional emission from crop burning in nearby states during October and November is the main contributing factor for increased pollution in this post-monsoon season. Furthermore, analysis reveals that cracker burning during festivals can also be considered as contributing factor to high M_{BC} for a short period in post-monsoon and winter seasons. Significant decrease in M_{BC} due to COVID-19 lockdown is also observed. M_{BC} in summer and monsoon are lower as compared to other seasons but are still higher than mean M_{BC} levels in several other urban cities of different countries. Also, the BC data obtained from nearby sites and Modern-Era Retrospective analysis for Research and Applications - version 2 (MERRA-2)'s surface black carbon (SBC) are compared against the M_{BC} to evaluate coherency among the different datasets, and discussed in detail.

Keywords: Black carbon, Delhi air pollution, Meteorology, Local emissions and regional transport, MERRA-2's surface black carbon

OPEN ACCESS

Received: March 27, 2022
Revised: May 12, 2022
Accepted: May 23, 2022

* **Corresponding Author:**
aggarwalsg@nplindia.org

Publisher:
Taiwan Association for Aerosol Research
ISSN: 1680-8584 print
ISSN: 2071-1409 online

1 INTRODUCTION

Increasing air pollution is one of the major challenges of the recent time in most of the metropolitan cities across the globe. Air pollution has become a serious health issue, especially in densely populated countries like India. The global burden of disease study in 2017 (Balakrishnan *et al.*, 2019), which was focused on analyzing the health effects of ambient air pollution in 195 countries found that 1.24 million (1.09–1.39 million) deaths in India during 2017 were attributable to air pollution. Another recent review study based on 59 studies (Rajak and Chattopadhyay, 2020) reported that long-term exposure to air pollution can be directly attributed to life-threatening conditions like asthma and heart attack.

According to a recent report on air quality (IQAir, 2020), out of 30 most polluted cities in the world, 22 are from India, and Delhi is rated the most polluted capital city in the world. Previous report has also found Delhi to be among the most polluted cities in the world (IQAir, 2019). Besides being the nation's capital, Delhi also harbors approximately 19 million people (16.8 million according to 2011 census), which further makes it an area of grave concern. Therefore, there is a long ongoing debate on causes and sources of high pollution levels in Delhi. Previous studies (Bikkina *et al.*, 2019; Kulkarni *et al.*, 2020; Liu *et al.*, 2018) suggest that crop residual burning in nearby states may be responsible for increased pollution levels. In addition to this, local emissions and meteorological conditions are also considered the other contributing factors for Delhi pollution (Tiwari *et al.*, 2014, 2013). Delhi also receives long-range transported dust from Middle East and Thar deserts in summer season (Kumar *et al.*, 2016).

Black carbon (BC) is an important air pollutant that forms a substantial part of PM mass and has its own spectrum of adverse health and climatic effects (Bond *et al.*, 2013; Mori *et al.*, 2020). Apart from undifferentiated PM mass, BC is considered as an additional standalone indicator of harmful particulate substance from combustion sources (Janssen *et al.*, 2011). Global carbon project report (Friedlingstein *et al.*, 2019) and various emission inventories (Bond *et al.*, 2007; Klimont *et al.*, 2017; Paliwal *et al.*, 2016; Wang *et al.*, 2012) have found India to be the second major contributor (after China) to global BC aerosol. However, these inventories contain large uncertainties in emission estimates of BC and there is a large discrepancy in BC emission estimates studies from India (Rana *et al.*, 2019). Therefore, ground-based observations of atmospheric BC are of utmost importance and a preferable source for measuring changes in emission estimates and investigating health and climatic implications of BC.

In India, openly accessible data of BC mass concentration (M_{BC}) is still limitedly available and researchers have to rely on independent observations. A recent review summarized the M_{BC} measurements in India based on the survey of 140 studies conducted in India spanning for a period from 2002 to 2018 (Rana *et al.*, 2019). It was found that long-term data on M_{BC} is scarce in India which makes it difficult to construct trend over the years and derive some meaningful information. Only few multi-year (3–5 year) studies have been conducted across the country (Gogoi *et al.*, 2013; Jose *et al.*, 2017; Kumar *et al.*, 2020; Sharma *et al.*, 2017; Talukdar *et al.*, 2015). Similarly, despite high relevance of long-term M_{BC} measurement studies in Delhi, very limited BC studies have been conducted in the previous decade and fewer are based on long-term (at least for 1 year) real-time data (Bisht *et al.*, 2015; Kumar *et al.*, 2020; Surendran *et al.*, 2013; Tiwari *et al.*, 2013; Tyagi *et al.*, 2020). Two of these studies were primarily focussed on realizing climatic effects of BC over Delhi (Bisht *et al.*, 2015; Surendran *et al.*, 2013). Kumar *et al.* (2020) evaluated the spatial and temporal heterogeneity of BC aerosol over India using three-year measurements from Indian Meteorological Department (IMD) BC observation network (one of the 15 observation sites is located in Delhi). Other two studies (Tiwari *et al.*, 2013; Tyagi *et al.*, 2020) were focussed on characterisation and comprising possible sources of BC aerosol in Delhi.

A recent review (Malik and Aggarwal, 2021) summarized the measurements technique used for real-time online measurement of BC levels in India and China. In India, most (> 95%) of the previous studies (where M_{BC} was measured using light absorption technique and not the evolved carbon technique) have made use of different versions of widely used instrument, i.e., Aethalometer (Malik and Aggarwal, 2021; Rana *et al.*, 2019). Multi Angle Absorption Photometer (MAAP) have been used in a single study (Hyvärinen *et al.*, 2010). The uncertainties of the M_{BC} measurements done in India by these instruments have not been evaluated quantitatively.

Table 1. Summary of all major events during measurement period.

S. No.	Event	Period	Source	Effect on M_{BC}
1	Diwali	October 27, 2019	Fireworks	Sudden increase in M_{BC} during celebration night leading to second largest peak in weakly averaged M_{BC} plot (see Fig. 4(b)).
2	Regional transport	October–November 2019	Crop-residue burning	M_{BC} in October increased nearly three times as compared to September (see Fig. 6(b)).
3	New Year	December 31, 2019	Fireworks	Sudden increase in BC levels during celebration night leading to largest peak in weakly averaged M_{BC} plot (see Fig. 4(b)).
4	Cold winter	December 2019–February 2020	Local open-burning	Increased local emissions along with non-favourable meteorological condition leading to highest daily M_{BC} in December and January (see Fig. 6(b)).
5	COVID-19 lockdown	March 25, 2020–April 9, 2020	Negligible sources	Averaged M_{BC} for 15 days before lockdown (3.42 ± 1.06 μg m^{-3}) is almost three times the averaged M_{BC} for 15 days into lockdown (1.18 ± 0.94 μg m^{-3}).

Considering this, we made measurements of M_{BC} using Continuous Soot Monitoring System (COSMOS) for the first time in India. The accuracy of M_{BC} measured by COSMOS is about 15%, as discussed in detail in following section. Since this is the first measurement in Delhi using COMSOS, comparison between M_{BC} and simultaneous BC measurement data obtained from nearby location (using Aethalometer, denoted as "M_{BC} (AE)" hereafter) is also performed. Also, Modern-Era Retrospective analysis for Research and Applications - version 2 (MERRA-2)'s surface black carbon (SBC) concentrations are compared with M_{BC}. MERRA-2's reanalysis data (SBC) have been used previously to define the spatial distribution and trends of BC and other pollutants in India and worldwide (Bali *et al.*, 2017; Evangeliou *et al.*, 2021; Navinya *et al.*, 2020; Qin *et al.*, 2019; Rana *et al.*, 2019; Sitnov *et al.*, 2020). Also, SBC data have been checked and evaluated against ground observations of BC in previous studies conducted outside India (Qin *et al.*, 2019; Xu *et al.*, 2020a). Malik and Aggarwal (2021) compared MERRA-2's SBC data with the ground observation's BC data published in previous peer reviewed studies conducted in India and China. However, a direct comparison between highly temporarily resolved datasets (as done by Qin *et al.* (2019) in Beijing) of SBC and ground observation has not been done in India.

In this study, we report M_{BC} measurements from September 2019 to August 2020 in Delhi, which can be recognised as a representative of eventful period. Measurement period spans various events like crop-residue burning in the months of October and November 2019 and a nation-wide lockdown due to COVID-19 pandemic during March–May, 2019. Furthermore, observation period covers major festive events (Diwali and New Year) which can be responsible for sudden peak in pollution concentration. Therefore, in this study, possible effects of these events and local meteorological conditions on the seasonal variations of M_{BC} are realized. Table 1 summarizes the major events during measurement period and their effects on M_{BC}. Based on the data analysis, we have tried to find the possible causes of severe air pollution in Delhi during the observation period. Information discussed here can be useful for better understanding of the Delhi's increasing air pollution and accordingly formulation of control strategy of carbonaceous aerosol.

2 METHODOLOGY

2.1 Site Description and Measurement Period

Black carbon (M_{BC}) measurement by COSMOS was made on the premises of the CSIR-National Physical Laboratory (NPL) located in New Delhi, India, (Fig. 1, 28.63°N and 77.17°E). NPL is surrounded by thinly populated Indian Agricultural Research Institute (IARI, PUSA institute) on three sides and a traffic (major rush hours are in morning and evening) road and residential area on one side. There is no major industry in nearby area which can affect local pollution levels. New Delhi, the capital of India, forms a small part of Delhi metropolitan area. Delhi is located in Indo-Gigantic Plain region spanning an area of 1,484 km^2. It is a landlocked city with the state of Haryana bordering it on three sides and Uttar Pradesh covering it from the fourth, i.e., East side.

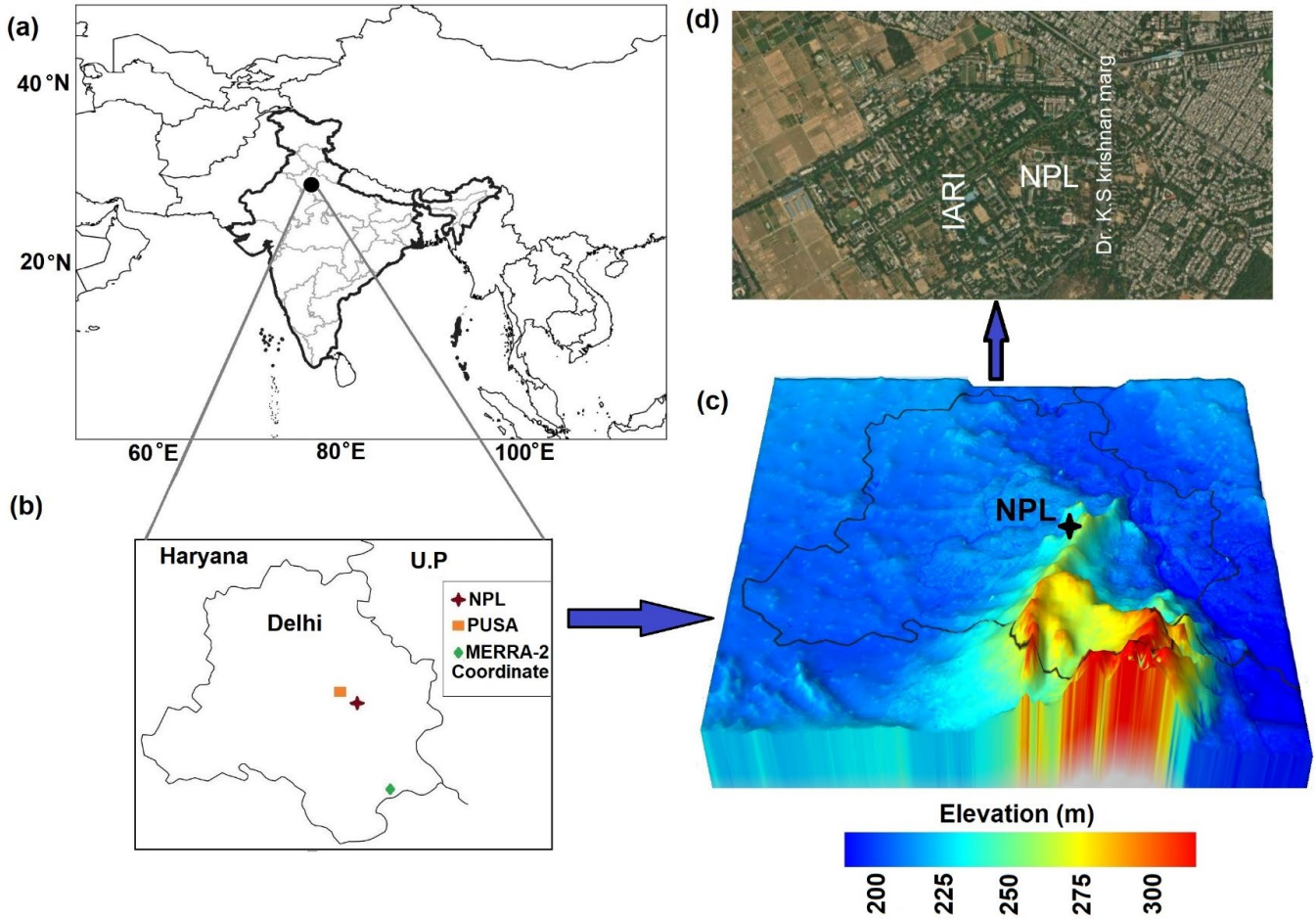

Fig. 1. Inset of world map showing (a) location of Delhi, location of measurement site, (b) nearby Aethalometer measurement site, and MERRA-2 coordinates which are used for comparison. (c) Digital elevation model map of Delhi is also included to show the role of its topography for low dispersion rate. Furthermore, (d) surrounding of measurement site is also shown to denote the urban location.

South-west monsoon is the most important feature controlling the Indian climate because about 75% of the annual rainfall is received during a short span of four months (June–September). So significant is the monsoon season to the Indian climate that the remaining seasons are often referred relative to the monsoon. According to the classification given by Indian Meteorological Department (Attri and Tyagi, 2010), India experiences four distinct seasons, i.e., winter, pre-monsoon, monsoon and post-monsoon. Monthly time span of each season is slightly different in different regions of country depending upon the arrival of monsoon and temperature variation. Year-round M_{BC} measurements were performed from September 2019 to August 2020 to cover all seasons in Delhi.

Fig. 2 shows monthly variation of meteorological parameters, i.e., ambient temperature (AT), relative humidity (RH), solar radiation (SR) and precipitation during measurement period. 24-Hourly averaged datasets of all parameters are taken from Central Pollution Control Board's (CPCB) Central Control Room for Air Quality Management website (https://app.cpcbccr.com). AT, RH and SR datasets of two monitoring station (Pusa-DPCC, Shadipur-CPCB) situated within 1.5 km radius of monitoring site are used to plot monthly variation. Precipitation data of monitoring stations, which are located near the sampling site were not available. Therefore, average of precipitation data of all monitoring stations (Alipur-DPCC, DTU-CPCB, Sirifort-CPCB) situated in Delhi are used. Ambient temperature was minimum during the months of December–February. Precipitation levels were maximum in the months of June–August. Therefore, seasons in Delhi are classified in general as—winter (December–February), pre-monsoon/summer (March–May), monsoon (June–August), and post-monsoon (September–November).

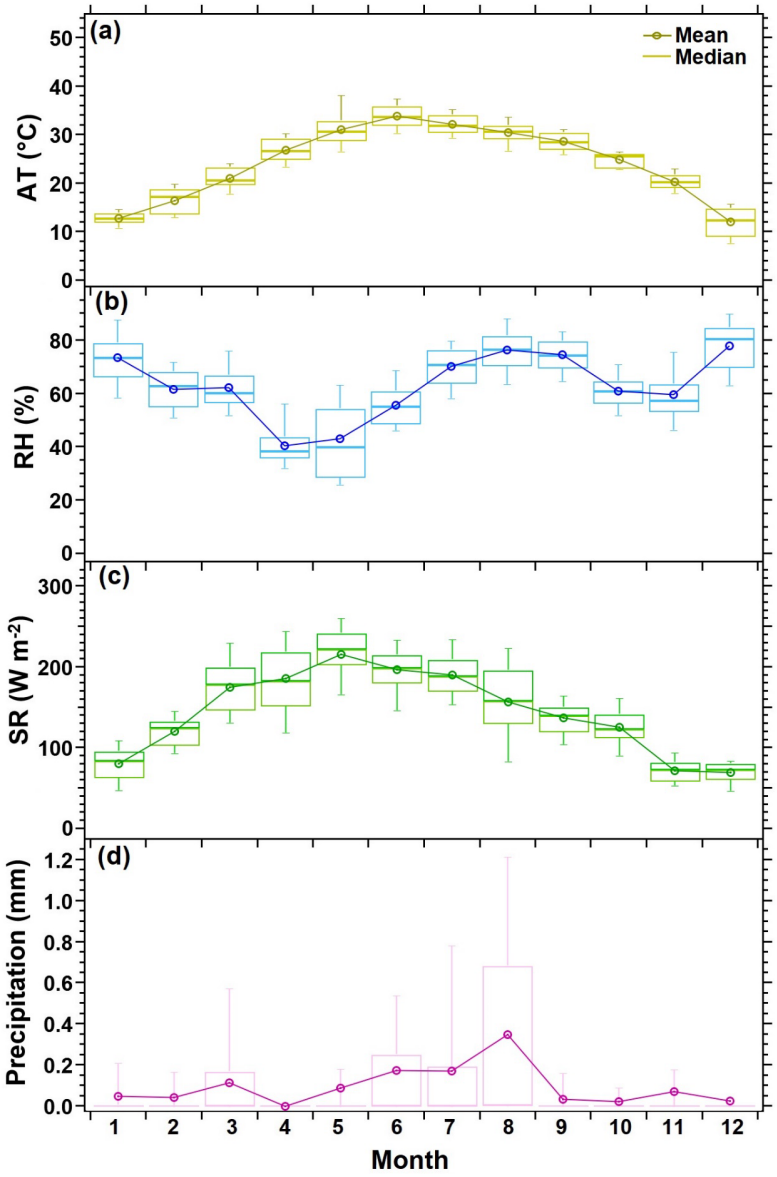

Fig. 2. Month wise variation of (a) ambient temperature (AT), (b) relative humidity (RH), (c) solar radiation (SR), and (d) precipitation. Mean values are denoted by circles and horizontal bold lines represents median value. For making these plots, 10, 25, 50, 75, 90 percentiles are used, i.e., 80% observations (10–90 percentile) lie between the whisker (vertical lines) and 50% (25–75 percentile) values lie within the box (same criteria are used for making all box plots in this paper).

2.2 Instrumentation

Details of the COSMOS are given in previous papers (Kondo *et al.*, 2011; Miyazaki *et al.*, 2008; Ohata *et al.*, 2021, 2019). In brief, the COSMOS measures the extinction coefficient (b_0) of aerosols collected on a quartz-fiber filter at a given wavelength (λ = 565 nm). High-efficiency particulate matter (HEPA) filters rolls were used in COSMOS for particle collection in this study. The inlet of the COSMOS is heated to 300°C to remove volatile light scattering particles and coating on BC particles. This excludes the effect on b_0 of co-existing volatile components externally or internally mixed with BC particles. The COSMOS is equipped with a PM_1 cyclone to minimize the effect in coarse mode of refractory non-BC particles, such as dust particles. Therefore, the absorption coefficient for the COSMOS is given as

$$b_{abs}(COSMOS) = f_{fil} b_0 \quad (1)$$

where, f_{fil} is a factor used to correct for the increase of absorption caused by multiple scattering in the filter medium (Bond *et al.*, 1999; Ogren, 2010; Ohata *et al.*, 2019). The mass absorption cross section (MAC) for the COSMOS ($m^2\ g^{-1}$) has been determined as

$$\mathrm{MAC(COSMOS,\ SP2)} \equiv \frac{b_{abs}(\mathrm{COSMOS})}{M_{BC}(\mathrm{SP2})} \tag{2}$$

where, the numerator and denominator, respectively, are simultaneous measurements of b_{abs} (Mm^{-1}) by COSMOS and M_{BC} ($mg\ m^{-3}$) by a single particle soot photometer (SP2) for ambient air. SP2 is based on laser induced incandescence technique (Malik and Aggarwal, 2021) and measures M_{BC} with an accuracy of about 10% (Kondo *et al.*, 2011; Moteki and Kondo, 2010; Ohata *et al.*, 2021). The MAC value for a HEPA filter at λ = 565 nm is about 9.25 ($m^2\ g^{-1}$) (Irwin *et al.*, 2015). M_{BC} (COSMOS) ($g\ m^{-3}$) at standard temperature (0°C) and pressure (101 kPa) can be estimated as

$$M_{BC}(\mathrm{COSMOS}) \equiv \frac{b_{abs}(\mathrm{COSMOS})}{\mathrm{MAC(COSMOS,\ SP2)}} \tag{3}$$

A "Standard COSMOS (Std-COSMOS)" was calibrated by comparison with the SP2 in Tokyo. Because the MAC of the Std-COSMOS was determined by comparison with SP2 (Eq. (2)), it acts as a transfer standard for the SP2. The b_{abs} (COSMOS) of each COSMOS manufactured is compared with the Std-COSMOS by sampling ambient BC particles in Osaka, Japan, typically for 1–2 weeks. The temperatures of the optical detector unit and filter holding unit of COSMOS are actively maintained at 50°C to minimize any possible effects of changes in ambient relative humidity (Kondo *et al.*, 2009; Miyazaki *et al.*, 2008). M_{BC} (COSMOS) was also compared with M_{BC} (SP2) at Hedo, located at downstream of the East Asian continent and at Ny-Ålesund in the Arctic (Ohata *et al.*, 2019). M_{BC} (COSMOS) and M_{BC} (SP2) agree to within about 10% at these sites, thus demonstrating the validity of using the Std-COSMOS to calibrate each of the COSMOS instruments to be used for field observations. It will be appropriate to estimate the absolute accuracy of M_{BC} (COSMOS) to be about 15%, including the 10% uncertainty of M_{BC} (SP2). This 15% uncertainty also covers the range of agreement between M_{BC} (COSMOS) and M_{BC} (SP2) previously reported by other groups at Ny-Ålesund (Zanatta *et al.*, 2018) and at Fukue, located downstream of the East Asian continent (Miyakawa *et al.*, 2017). Hereafter we denote M_{BC} to represent M_{BC} (COSMOS) for simplicity.

2.3 Additional Data Set

Black carbon data of a nearby monitoring station (station name "PUSA, Delhi-IMD", location denoted as PUSA in Fig. 1(b)), available at CPCB's website (https://cpcbccr.com/) are used for comparison with M_{BC} measured at NPL in this study. Mass concentrations of black carbon at monitoring station of PUSA are measured using Aethalometer (Hansen, 2005; Sedlacek, 2016) with $PM_{2.5}$ cutoff size inlet. Absorption coefficient measured by Aethalometer (AE) at a wavelength of 880 nm was converted to BC mass concentration M_{BC} (AE) by assuming a mass absorption cross section (MAC) of 7.7 $m^2\ g^{-1}$. It is important to note that information about Aethalometer MAC calibration, i.e., whether the calibration is at STP as it is done for COSMOS is unknown.

NASA's MERRA-2 reanalysis data (SBC) over Delhi available through publicly accessible website (https://disc.gsfc.nasa.gov/datasets?project=MERRA-2) are also used for the comparison with M_{BC}. MERRA-2 is the latest long-term global atmospheric reanalysis to assimilate space-based observations of aerosols and represent their interactions with other physical processes in the climate system initiated by NASA's Global Modeling and Assimilation Office (GMAO). Details about MERRA-2 dataset can be accessed from previous studies (Bali *et al.*, 2017; Bosilovich *et al.*, 2016; Buchard *et al.*, 2015; Kuo, 2017). Different type of aerosols (including BC) is simulated using the Goddard Chemistry Aerosol Radiation and Transport module in GEOS-5 (Bali *et al.*, 2017; Buchard *et al.*, 2015). Surface black carbon data obtained from MERRA-2 of coordinates 28.5°N and 77.25°E, which are closest to measurement site's coordinates, i.e., 28.63°N and 77.17°E are used for comparison.

Hourly data of boundary layer height (BLH) was obtained from the climate data store (https://cds.climate.copernicus.eu/cdsapp#!/dataset/reanalysis-era5-single-levels?tab=form). Ventilation coefficient (VC) is an important parameter to define the dispersion of a pollutant at a

place. It is calculated as the product of average BLH and average wind speed (WS) over a given area. The spatial resolution of gridded BLH data source is 0.25° × 0.25° (approximately 30 km^2). Therefore, hourly averaged WS data of 28 monitoring stations in Delhi is used to cover the area spanned by BLH data grid. This monitoring station network is jointly operated by the Central Pollution Control Board (CPCB), Delhi State Pollution Control Committee (DPCC), the Indian Institute of Tropical Meteorology (IITM), and the IMD. Open source archived fire map data from NASA's Fire Information for Resource Management (FIRMS, Data source-VIIRS) website is utilized for fire spots analysis. Furthermore, Global Data Assimilation System (GDAS) meteorological data files (1° × 1° resolution) are used to calculate the air mass back trajectories.

3 RESULTS AND DISCUSSION

3.1 Data Comparisons

3.1.1 Comparison between M_{BC} and BC concentration of nearby monitoring station i.e., M_{BC} (AE)

Fig. 3(a) shows the scatter plot of 24-hour averaged M_{BC} (AE) at PUSA site (Fig. 1) against M_{BC}. M_{BC} (AE) data correlate very well with the M_{BC}, where correlation coefficients (r) increase with the increase in averaging time period. For hourly, daily, and monthly averaged data, r values are 0.81, 0.89, and 0.96, respectively. Although M_{BC} at NPL site correlate well with the M_{BC} (AE) of PUSA site, there is a bias between both the datasets. Furthermore, the bias between two data set is larger at higher concentrations. Slope of the linearly fitted line for $M_{BC} < 8$ μg m^{-3} is 0.88 which is closer to 1 than that for all data points (0.67). This might be due to systematic bias between different instruments used (Aethalometer at PUSA and COSMOS at NPL) for deriving BC concentrations.

Ohata *et al.* (2021) made direct comparison of COSMOS and Aethalometer in the Arctic and determined MAC there. However, no such comparisons have been made, especially for urban site and MAC of Aethalometer is poorly characterized. Because, it is difficult to estimate the uncertainties of M_{BC} (AE) at PUSA site, the comparison of Aethalometer with COSMOS is rather qualitative this time. We used currently available M_{BC} (AE), although direct and systematic comparisons as done elsewhere (Ohata *et al.*, 2021) are important and needed, especially under high BC mass loading condition (urban sites). Nevertheless, the good correlation between both sites suggests that the NPL site can be considered as representative for the temporal variations of BC aerosol in Delhi area.

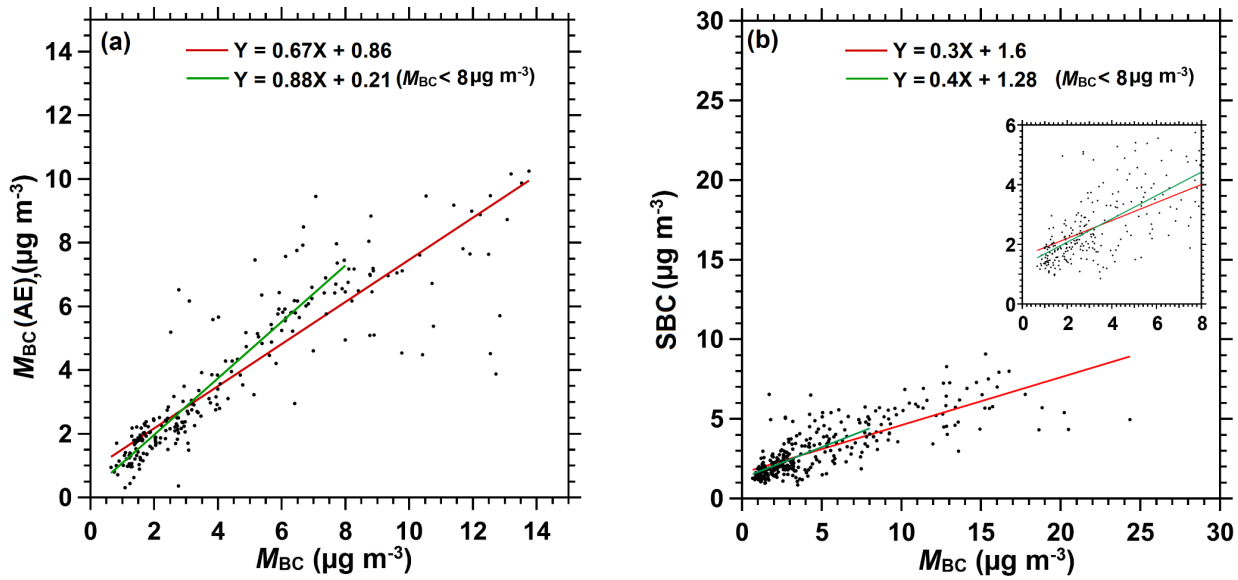

Fig. 3 Scatter plot of 24-hour averaged M_{BC} (AE) at (a) PUSA and (b) SBC against M_{BC}. Inset figure shows the relation between SBC and $M_{BC} < 8$ μg m^{-3}.

3.1.2 Comparison between M_{BC} and SBC

The SBC data are compared with 24-averaged M_{BC} for the complete observation period, i.e., September 2019–August 2020. The correlations of the two data sets are shown in Fig. 3(b). SBC data correlate well with the M_{BC}, where correlation coefficients increase with increase in averaging time period. The *r* values for hourly, daily, and monthly averaged data are 0.57, 0.79, and 0.93, respectively.

Mean SBC concentration for the complete observation period is 3.07 μg m^{-3} which is about 60% of mean M_{BC} (5.02 μg m^{-3}). Also, the scatter plot of 24-hour averaged SBC against 24-hour averaged M_{BC} (Fig. 3(b)) shows that MERRA-2 underestimates the BC concentration, whereas the correlation between these data is fairly good, i.e., r = 0.79. As shown in Fig 3(a), the slope of the linearly fitted line of data between M_{BC} (AE) and $M_{BC} < 8$ μg m^{-3} is better (0.88) than that for all the data points (0.67), inset Fig. 3(b) also suggests that the slope of linearly fitted line for $M_{BC} <$ 8 μg m^{-3} is 0.4, which is slightly better than that of the slope with all the data points, i.e., 0.3. This further indicates that underestimation of BC concentration by MERRA-2 is more pronounced at higher concentration. Similarly, Navinya *et al.* (2020) also showed that MERRA-2 generally underestimates the $PM_{2.5}$ in terms of both the mass concentration and the number of exceedance days, i.e., when 24-hour averaged air quality index (AQI) values exceeded the AQI limits of "Good" category as per national ambient air quality standards (NAAQS) of India. However, on the contrary, studies conducted in Beijing found MERRA-2 to be overestimating BC concentration (Qin *et al.*, 2019; Xu *et al.*, 2020b).

One of the reasons for bias between two datasets can be the uncertainties in the emission estimates which are used as input to MERRA-2 for simulating the BC aerosol. Other reasons may be the difference in spatial resolution of both datasets (i.e., SBC and M_{BC}). The spatial resolution of MERRA-2 data set is 0.5° × 0.625°, hence one rectangular grid (made up of 4 data points) of MERRA-2 data set covers a large area (about 50 × 50 km^2). Therefore, it can be deduced that one coordinate/point of MERRA-2 gridded dataset represents SBC levels roughly over an area of 15 × 15 km^2. On the other hand, M_{BC} ideally represents BC levels measured at one site. As mentioned earlier, SBC concentration of data point whose coordinates (28.5°N, 77.25°E) were nearest to the NPL site are used for comparison in current study (Fig. 1(b)). The linear distance calculated between the NPL site and MERRA-2's data point is roughly 12–15 km and pollution levels at ground can change considerably over such distance in Delhi where local pollution sources are distributed heterogeneously.

Overall, the correlation between the MERRA-2's data and M_{BC} is moderate which is good enough to suggest representativeness of measurement site. A comparison between mean M_{BC} levels of several sites covering entire area under one grid of MERRA-2 dataset would be more appropriate for further assessment and understanding the deviation between both the data sets.

3.2 Year-Round Concentration of BC

Here, we discuss year-round concentration of M_{BC} measured using COSMOS (i.e., temporal variation in Delhi). Fig. 4 shows 1-hour averaged, 24-hour averaged and weekly averaged plots of M_{BC} measured for one-year starting from September 1, 2019 to August 31, 2020. However, data for almost one month from April 9, 2020 to May 13, 2020 are not available due to COVID-19 lockdown. 24-Hour averaged M_{BC} for the complete observation period varied from 0.7 to 29.1 μg m^{-3} with a mean value of 5.02 ± 4.40 μg m^{-3}. Table S1 summarizes short term as well as long-term studies conducted in Delhi in the past decade (2011–2020). M_{BC} observed in current study is significantly lower than those reported by recent studies (12.73 μg m^{-3} and 13.57 μg m^{-3}) conducted in Delhi for the time period 2016–2018 (Kumar *et al.*, 2020; Tyagi *et al.*, 2020). Possible reasons for the difference might be different study time period and use of different instruments (AE-33 in Tyagi *et al.* (2020) and Kumar *et al.* (2020), and COSMOS in current study), use of different PM mass for BC measurement ($PM_{2.5}$ in Kumar *et al.* (2020) and PM_1 in current study), and difference in sampling sites as air pollution levels in Delhi are not homogenous. However, observed concentration is comparable to those reported by other studies conducted in the year 2011 (6.7 μg m^{-3}) and 2011–2012 (7 μg m^{-3}) (Bisht *et al.*, 2015 and Tiwari *et al.*, 2013, respectively). It is noteworthy that these studies were conducted at a site (IITM) which is ~1 km away from measurement site of current study.

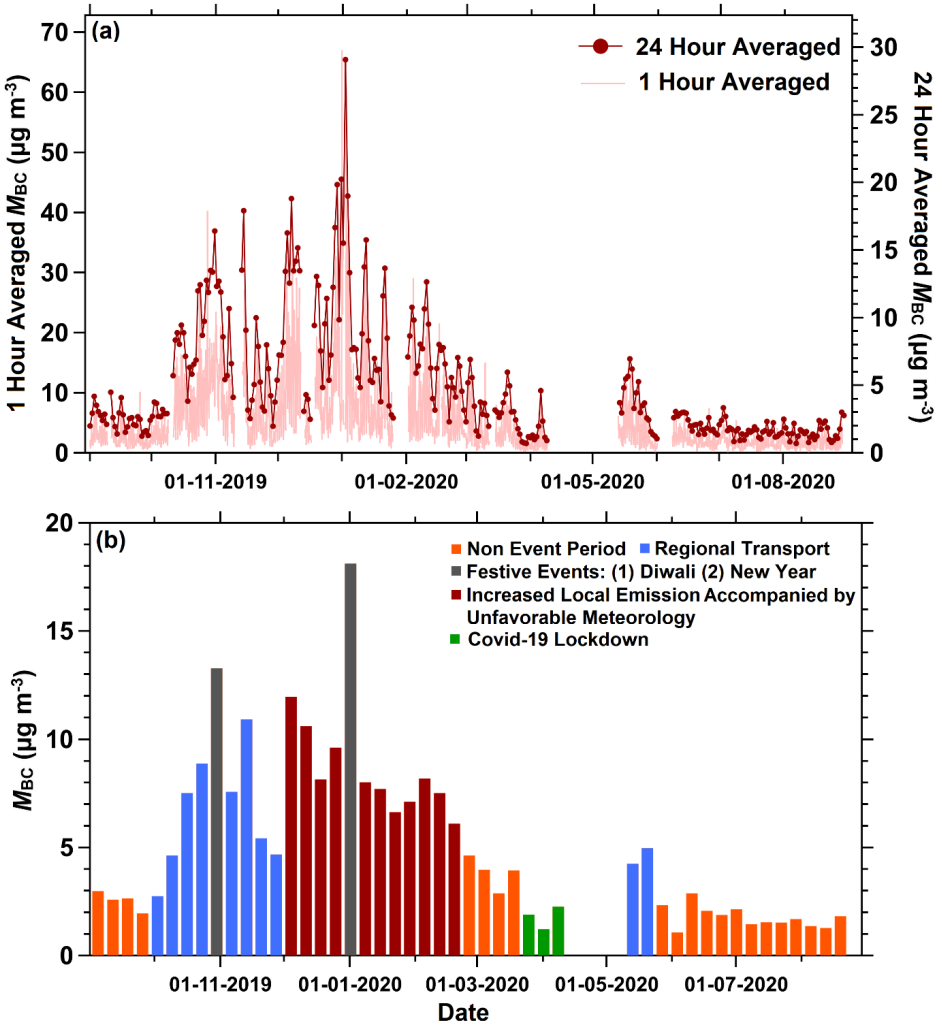

Fig. 4. Temporal variation of M_{BC}: (a) 1-hour, 24-hour, and (b) weekly averaged. All the events are highlighted by color coded bars in weekly averaged plots and are discussed in details in text.

In this study, maximum value of 24-hour averaged M_{BC} reached up to 29.1 µg m^{-3} on January 2, 2020, i.e., one day after the New Year celebration. Minimum value of 24-hour averaged M_{BC} went down to 0.7 µg m^{-3} on March 29, 2020, i.e., one week into the COVID-19 lockdown in India (Fig. 4(a)). Also, Fig. 4(b) shows several events (highlighted by colored bars) those influenced BC concentration significantly during the observation period. These events are further discussed in the following sections.

3.3 Diurnal Variation

For better understanding on the day- and night-time atmospheric chemistry, conditions and sources of BC, here we discuss diurnal variation of M_{BC} for the measurement period. Fig. 5 shows 1-hour averaged time series of diurnal variation for complete observation period. Mean day-time M_{BC} (0600 h–1800 h, LT) is 3.99 ± 3.42 µg m^{-3} which is lower as compared to night-time mean value of 6.01 ± 5.8 µg m^{-3} (1800 h–0600 h). Wilcoxon rank test at significance level of 0.05 is performed to test the significance of difference between day-time and night-time concentration. Significantly higher M_{BC} at night-time indicates a possible influence of increased emissions due to heavy-duty diesel vehicles whose entry is allowed only after 2200 h in Delhi.

Diurnal plot (Fig. 5) shows a slight elevation in M_{BC} during morning (0700 h–0900 h) and evening (1900 h–2100 h). Similar diurnal variation pattern has been observed in previous studies as well (Srivastava *et al.*, 2014; Tiwari *et al.*, 2013). Diurnal plots of boundary layer height (BLH), wind speed (WS) and ventilation coefficient (VC) over Delhi are given in Fig. S1. Diurnal variation

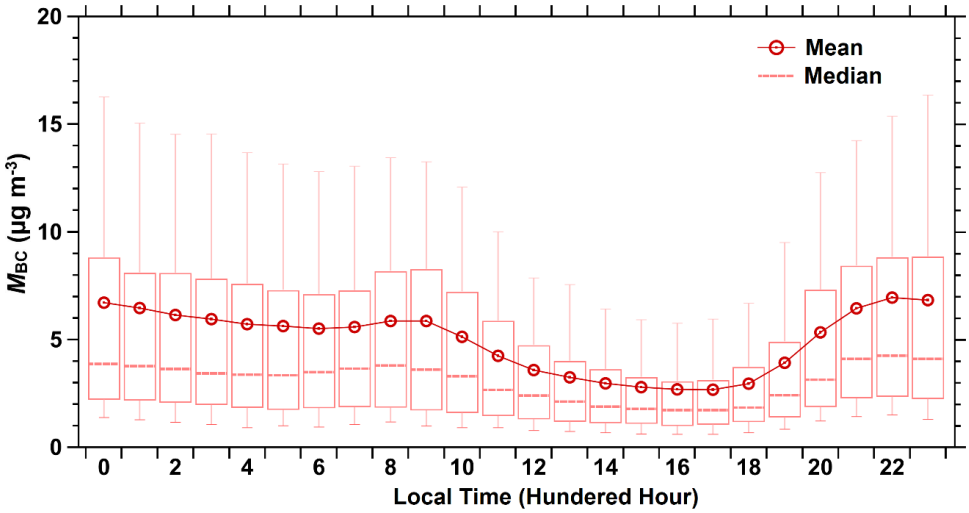

Fig. 5. Box and whisker plots showing diurnal variation of M_{BC} throughout the observation period.

of M_{BC} during observation period showed negative correlation with diurnal variation of BLH (r = –0.88 for n = 24), WS (r = –0.72 for n = 24) and VC (r = –0.86 for n = 24) indicating the dominance of dispersion factor. Same is depicted from diurnal plots as distinctive rise in WS, BLH and VC plots during afternoon also coincide with dip in M_{BC}. However, during morning hours (0700 h–0900 h), the mean M_{BC} increases despite increase in dispersion parameters. This anomaly is possibly due to the effects of increased traffic on nearby road during these peak hours.

3.4 Seasonal and Monthly Variation

Year-round M_{BC} data is further categorized for winter, summer, monsoon and post-monsoon seasons in Delhi. These seasonal as well as month-wise variations of M_{BC} are shown using box and whisker plots in Fig. 6. The highest concentration of M_{BC} is observed in winter (daily mean = 8.9 ± 4.94 µg m^{-3}) followed by post-monsoon (daily mean = 5.72 ± 3.96 µg m^{-3}), whereas monsoon is the least polluted among all seasons (daily mean = 1.76 ± 0.63 µg m^{-3}). M_{BC} in summer and monsoon are significantly lower than post-monsoon and winter and comparable to other Asian urban cities (Chen *et al.*, 2016; Kumar *et al.*, 2020; Sahu *et al.*, 2011; Zhang *et al.*, 2020). However, these values are still higher than the yearly mean M_{BC} levels reported for some developed countries (Crilley *et al.*, 2015; Healy *et al.*, 2017; Mousavi *et al.*, 2018; Saha and Despiau, 2009).

This variation (trend) in M_{BC} is in accordance with previous studies listed in Table S1 (Bisht *et al.*, 2015; Srivastava *et al.*, 2014; Tiwari *et al.*, 2013; Tyagi *et al.*, 2020). Low wind speed and

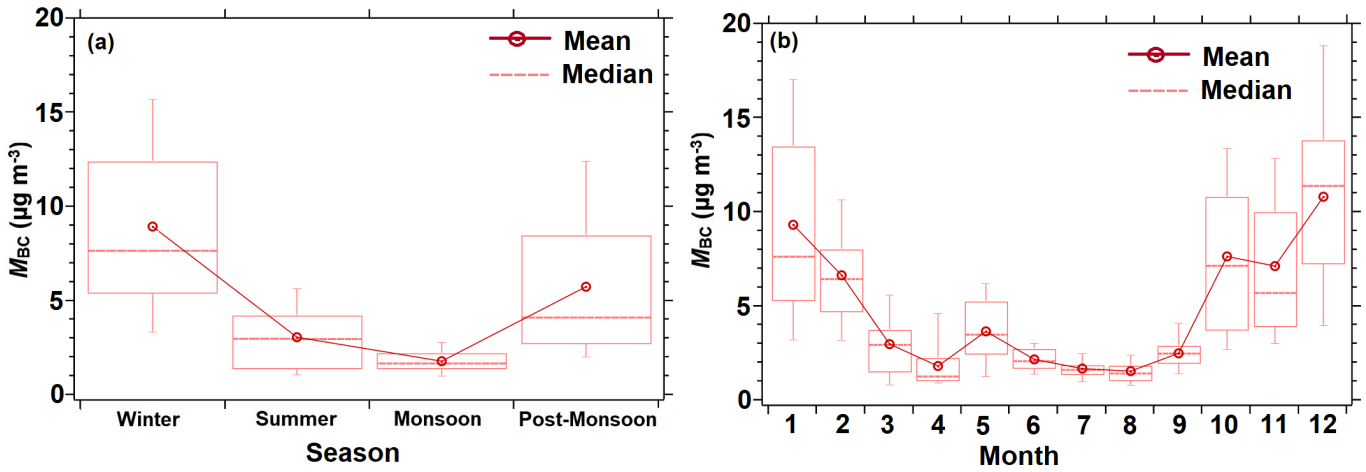

Fig. 6. Box and whisker plots showing (a) seasonal and (b) monthly variation of M_{BC}.

shallow mixed layer were found to be main reasons for high levels in winter (Tiwari *et al.*, 2013). Furthermore, dominance of local emission in winter of 2015–2016 has been shown by Dumka *et al.* (2018). Non-local fire emissions were reported to be contributing to about 20% of particulate matter mass in October and November (post-monsoon) (Kulkarni *et al.*, 2020). Moreover, India celebrates a number of different festivals owing to its diverse demography, and festivals are key to the respective cultures. Diwali is one of such festivals, which is celebrated throughout the country. While it started off as a festival of lights, the celebration practice has taken a turn for the worse in the post-industrial era with the introduction of chemical fireworks (crackers). Various previous studies have highlighted the worse effect of cracker burning on air quality during the night of Diwali (Ghei and Sane, 2018; Mukherjee *et al.*, 2018; Rao *et al.*, 2012). Following these approaches and findings, further analysis and observation report of seasonal and monthly variation are discussed in following subsections.

3.4.1 Role of local meteorology

Here, we discuss the effect of local meteorological conditions on M_{BC} at measurement site. As mentioned earlier, monthly variations of 4 meteorological parameters (i.e., AT, RH, SR and precipitation) near to measurement site are shown in Fig. 2. Further, monthly variations of critical parameters (BLH, WS, VC) are shown in Fig. 7, which suggest an idea about dispersion factor

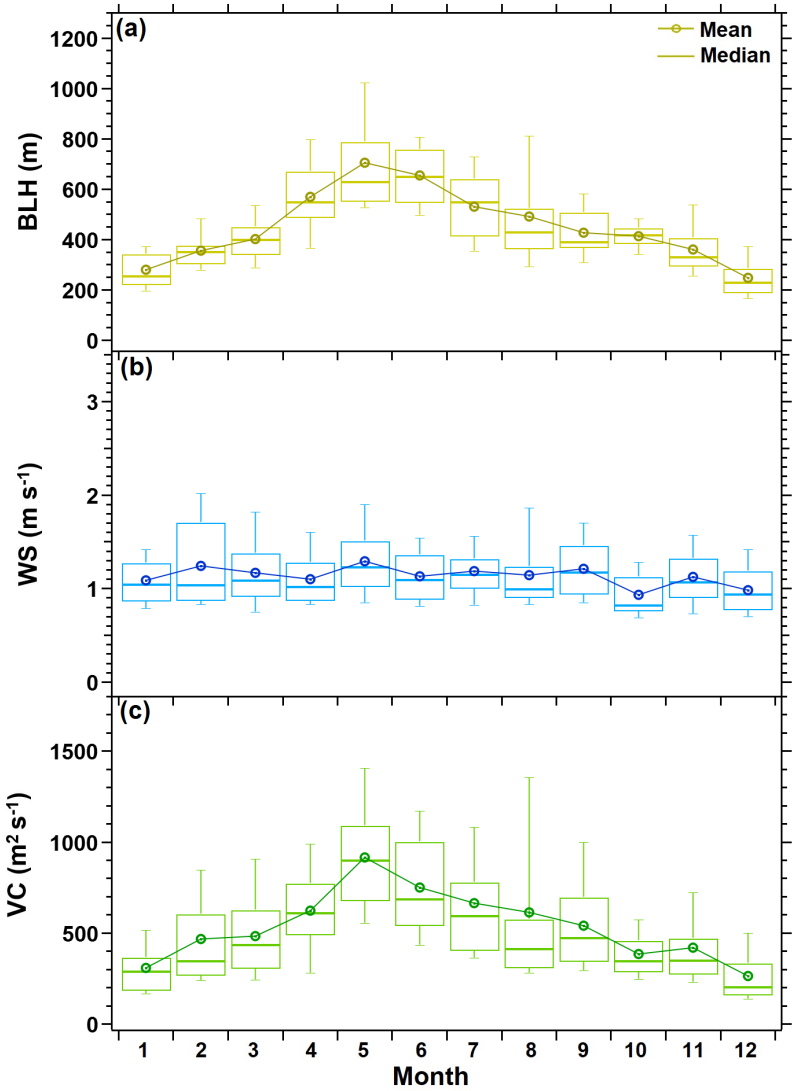

Fig. 7. Monthly variation of (a) boundary layer height (BLH), (b) wind speed (WS), and (c) ventilation coefficient (VC) over Delhi.

Table 2. Correlation coefficient (r) between M_{BC} and meteorological parameters and fire spots.

Parameter	Correlation (r, for n = 307) with 24-hour averaged M_{BC} (μg m^{-3})	Correlation (r, for n = 12) with monthly averaged M_{BC} (μg m^{-3})
Ambient temperature (°C)	–0.61	–0.83
Relative humidity (%)	0.08	0.30
Solar radiation (W m^{-2})	–0.56	–0.84
Precipitation (mm)	NA (Not Applicable)	–0.51
Wind speed (m s^{-1})	–0.47	–0.68
Boundary layer height (m)	–0.47	–0.68
Ventilation coefficient	–0.48	–0.74
Fire spots (km^{-2})	NA	0.35 (all months) 0.81 (excluding December and January)

over Delhi. Table 2 summarizes the dependency of 24-hour averaged as well as monthly M_{BC} on meteorological parameters. 24-Hour averaged M_{BC} showed moderate negative correlation (ranging from –0.47 to –0.60) with all meteorological parameters except RH. Similarly, month wise M_{BC} shows strong negative correlations (ranging from –0.51 to –0.84) with all meteorological parameters except RH. There exists negligible (24-hour averaged) to low correlation (monthly) between RH and M_{BC}. It was reported that variation in ambient RH can affect the BC measurements of filter-based instruments as MAC value increases with increase in RH (Wu *et al.*, 2016). The temperatures of the optical detector unit and filter holding unit of COSMOS are controlled at 50°C (Section 2.2). This, together with the heated inlet stabilizes the moisture content in the aerosol at the time of measurement, consequently no effect of RH in measurement as such is predicted.

Strong negative correlations between month wise variation of meteorological parameters and M_{BC} show the dominance of local meteorology and local sources in defining the M_{BC} over Delhi. High values of meteorological parameters in monsoon and summer favors low M_{BC}, whereas unfavorable meteorological conditions (i.e., low BLH, VC and AT) during winter can be directly attributed to high M_{BC}.

Furthermore, Delhi's topography also plays an important role in enhancing the impact of meteorology. As visible in digital elevation model map (Fig. 1(c)), Delhi's surface is distinctively uneven with elevation above sea level varying from nearly 200 m to > 300 m. Most of the landmass has elevation in the approximate range of 190–230 m which is surrounded by hills (significantly elevated (280–320 m) surface) at South-East and Southern part. Sometimes during winters, the 24-hour averaged BLH is observed to be as low as 100 m above ground, and in such cases pollutants accumulate in atmosphere over Delhi. Apart from regional pollution comes when winds are North-Westerly, for local pollution also these hills play a role of wall to trap the pollutants over Delhi. So, during these low BLH and calm conditions, the dispersion rate becomes very low which leads to high pollution levels.

Strongly correlated (with M_{BC}) meteorological parameters (AT, SR, BLH, VC) show smooth increment from January to mid of the year (May–June) and then smooth decrement from mid-year to December. However, monthly variation plot of M_{BC} is not so smooth and there are non-linearity and deviations as compared to plots of meteorological parameters. All three months (September, October, and November) in post-monsoon experiences similar meteorological conditions, whereas M_{BC} are significantly higher in October and November as compared to September. Similarly, May has more favorable meteorological conditions as compared to June and April but M_{BC} is higher than June and April. Furthermore, there is a sudden increment in M_{BC} from November to months of December and January (Fig. 6(b)), whereas there is smooth decrement in meteorological parameters from November to January (Fig. 7). These anomalies are indicative of change in local as well as regional emissions due to different events which are further explained in following subsections.

3.4.2 Regional emission transport

The 48 hours air mass back trajectories arriving up to 1000 m above sampling site for the month of September and October are shown in Fig. 8. Air mass back trajectories from GDAS

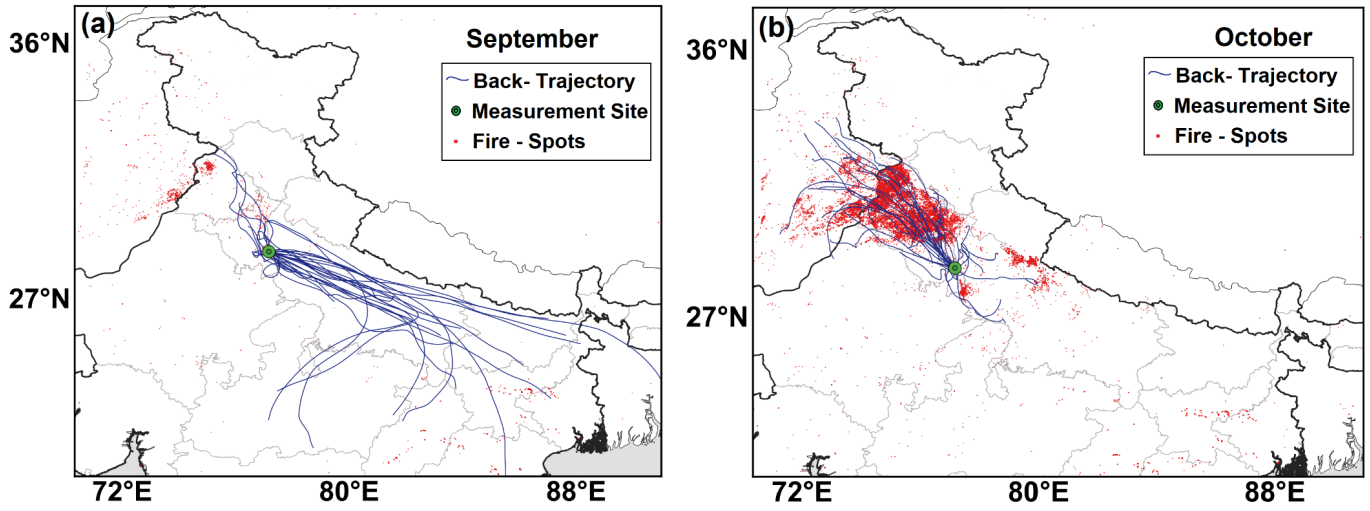

Fig. 8. Maps showing air mass back trajectories and fire spots in nearby areas of Delhi for the months of (a) September, and (b) October.

meteorological files are calculated using geographic information system (GIS) based software, "TrajStat". 48-Hour back trajectories are calculated for each day (refresh time of 0600 hours, LT). Additionally, fire spots "shapefiles" from FIRMS are loaded using QGIS for combined fire spots and air mass back trajectory analyses.

In September (mean M_{BC} = 2.49 ± 0.89 μg m^{-3}) most of the air masses at sampling site are arrived from South-East direction where there are very few fire spots. Whereas in October (mean M_{BC} = 7.63 ± 3.87 μg m^{-3}), most of the air masses at sampling site arrived from North-West direction where large number of fire spots are visible as compared to the month of September. Similar maps are drawn for other months (Fig. S2). Using these maps, monthly mean number of fire spots per unit area are calculated for each month using Eq. (4).

$$F_{av} = \frac{F_t}{A \times N} \tag{4}$$

where, F_{av} is monthly mean number of fire spots per unit area (km^{-2}), F_t is total number of fire spots on 48 hours back trajectories area for the complete month, A is the total geographical area spanned by 48 hours back trajectories (km^2) and N is total number of observation days in corresponding month.

Fig. 9(a) shows the relation between number of monthly averaged fire spots per unit area (F_{av}) and corresponding M_{BC}. In general, M_{BC} correlates very well with F_{av} except for the months of December and January (Table 2). From Fig. 9(a), it is evident that elevated M_{BC} during the months of October and November in post-monsoon despite having comparable meteorological conditions in September (Fig. 2 and Fig. 7) is due to increased fire spots in nearby areas/states of Delhi. Similarly, spike in F_{av} during month of May is also responsible for elevation of M_{BC}. However, in May, effect of fire spots is less compared to that in October and November as meteorological conditions are favorable (relatively high BLH, VC and WS) in May. In the months of May, October and November, increased fire spots are due to crop-residue burning in nearby states (mainly Haryana, Panjab and Uttar Pradesh) of Delhi (CREAMS; http://creams.iari.res.in/cms2/index.php).

3.4.3 Increased local emissions in winter

As discussed previously, there is a sudden increment in M_{BC} from November to months of December and January (Fig. 6(b)) whereas there is smooth decrement in meteorological parameters from November to December. Also, monthly mean fire spots per unit area in winter are less as compared to months of post-monsoon season (October, November) and are comparable to monsoon and summer seasons. Delhi faces severe cold during the months of December and

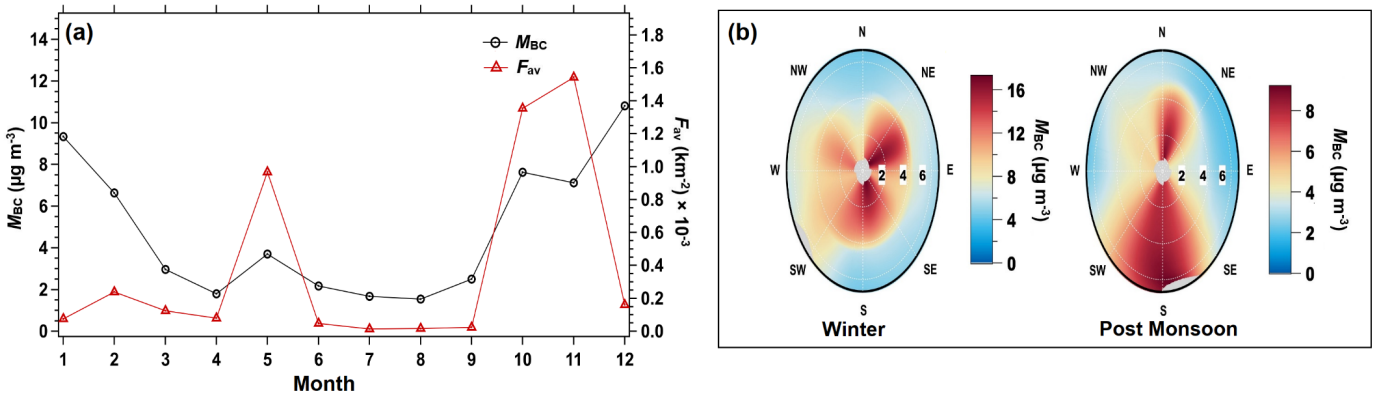

Fig. 9. (a) Monthly averaged fire spots per unit area in the trajectory path showing effect of fire counts in the months of May, October and November, also (b) NWR analysis for post-monsoon and winter season showing dominance of local emission during winter.

January with average temperature drops as low as 2–3°C during night-time. The daily mean temperature for the months of December and January (Fig. 2(a)) near to measurement site was 12.5°C and 13.3°C, respectively. Moreover, Delhi receives cold waves from the nearby Himalayas resulting in lower apparent temperature as an impact of wind-chill. Therefore, open burning (including waste, wood, coal and biomass) to fight severe cold in winters is a common practice followed by people in Delhi (Kumar *et al.*, 2018). Therefore, combined effect of increased local emission due to open burning and non-favorable meteorological conditions can be the major reason for sudden increment in M_{BC} in winter.

In Fig. 9(b), Non-Parametric Wind Regression (NWR) analysis results show that in winter very high M_{BC} are associated with low wind speed (< 4 km s^{-1}) showing the dominance of local sources. Whereas, in post-monsoon high M_{BC} are associated with high as well as low wind-speed showing the effect of regional transport of aerosols. Non-Parametric Wind Regression (NWR) analysis is performed using ZeFir (Petit *et al.*, 2017), which is an IGOR-based package that provides user friendly coupling between pollutant concentrations and wind data. Non-parametric Wind Regression techniques couple wind data (direction and/or speed) with pollutant concentration to alternatively highlight wind sectors that are associated with high measured concentrations (Henry *et al.*, 2009).

Furthermore, month wise variation plot of M_{BC} (Fig. 6(b)) shows that in winter, M_{BC} are significantly higher in December and January as compared to February. This observation is also indicative of increased emission due to open burning by local people during months of December and January which are colder in comparison to February. Qualitative impact of increased local emission during cold winters has been realized previously in Delhi (Dumka *et al.*, 2018). Effect of residential coal burning and relatively stable meteorological conditions during winters were found to be the possible reason for increment in M_{BC} in Beijing as well (Chen *et al.*, 2016; Liu *et al.*, 2016). However, a rigorous chemical analysis and survey-based study is required to quantify and further investigate the effect of open burning in winter.

3.4.4 Impact of festive events

Cracker-burning during Diwali has been prevalent for a long time and its impact on pollution levels in Delhi have been observed in previous studies (Sateesh *et al.*, 2018; Singh and Srivastava, 2020). During Diwali festival of 2019 also, the crackers were observed to be burnt and weekly averaged M_{BC} rose significantly around this festival (peak 1 in Fig. 4(b)). Fig. 10 shows the diurnal variation of M_{BC} on the days of Diwali and New Year. Diurnal characteristics for these two days are distinguishable from that of whole year (Fig. 5), where hourly averaged M_{BC} throughout night hours (1800 h–0600 h, LT) are similar. Unusual and nearly identical sharp peak around midnight on New Year as well as Diwali are clear indicative of cracker burning on these days. Therefore, in the recent years, the practice of cracker burning has transcended beyond the day of Diwali and events like New Year's Eve also witness a significant amount of cracker burning.

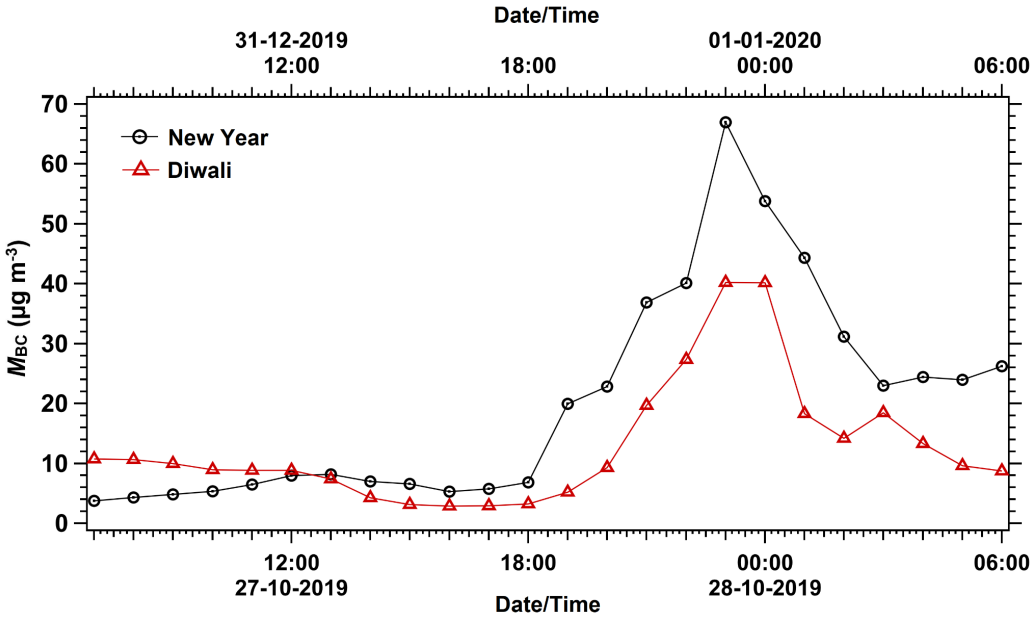

Fig. 10. 1-Hour averaged M_{BC} time series during Diwali and New Year festivals.

During Diwali (post-monsoon), weekly averaged M_{BC} (peak 1 in Fig. 4(b)) is comparable to nearby weekly averaged M_{BC}, whereas during New Year (winter), weekly averaged peak (peak 2 in Fig. 4(b)) is significantly higher from nearby weekly averaged concentrations. Comparable levels of weekly averaged M_{BC} during Diwali in post-monsoon indicates that pollution from local emissions gets dispersed easily and doesn't affect M_{BC} significantly during post-monsoon. However, in winter, distinctive weekly averaged M_{BC} peak around New Year shows the significant role of amplified effect of local meteorology on local emissions as dispersion of local pollution becomes non-favorable in winter (as discussed above). Furthermore, the number of weddings conducted in winters are significantly higher than other seasons as Indian culture relies heavily on astrology and most auspicious days fall in winter. Therefore, celebrations by cracker burning in weddings as well may also lead to increase the emissions.

3.4.5 BC in COVID-19 lockdown period

India went into first phase of nation-wide lockdown for 21 days from March 25, 2020 to fight the COVID-19 pandemic. All the industrial activity and traffic movement except essential services were prohibited. As a result, unprecedented low levels of pollution were seen in Delhi and throughout India (Dhaka *et al.*, 2020; Mahato *et al.*, 2020). In this study, the impact of COVID-19 lockdown on BC concentration at measurement site are analysed. Following a similar approach as in previous study where the effect of COVID-19 lockdown on $PM_{2.5}$ levels in Delhi has been analysed by comparing data of 7 days before and 7 days into lockdown (Dhaka *et al.*, 2020), in this study also M_{BC} for continuous 15 days before (March 10–24, 2020) and 15 days after (March 25–April 8, 2020) the implementation of lockdown are considered for analysis.

Fig. 11 shows the day wise (one month) variation of M_{BC} from March 10th to April 8th. The average M_{BC} during 5th April night was about three times higher than the previous night due to nationwide light candles and firecrackers, and thus M_{BC} data for these two days were excluded from our analysis. Averaged M_{BC} for 15 days before lockdown (3.42 ±1.06 µg m^{-3}) is almost three times the averaged M_{BC} for 15 days into lockdown (1.18 ± 0.94 µg m^{-3}). Wilcoxon rank test at significance level of 0.05 is performed to check the significance of difference in mean. BC data from April 9, 2020 to May 13, 2020 could not be recorded due to instrument failure as it could not be attended in lockdown. Therefore, effect of complete lockdown period on M_{BC} cannot be realized. Nevertheless, significant decrease in M_{BC} during 15 days into lockdown can be considered a contributing factor to lower M_{BC} in summer of 2020 in Delhi.

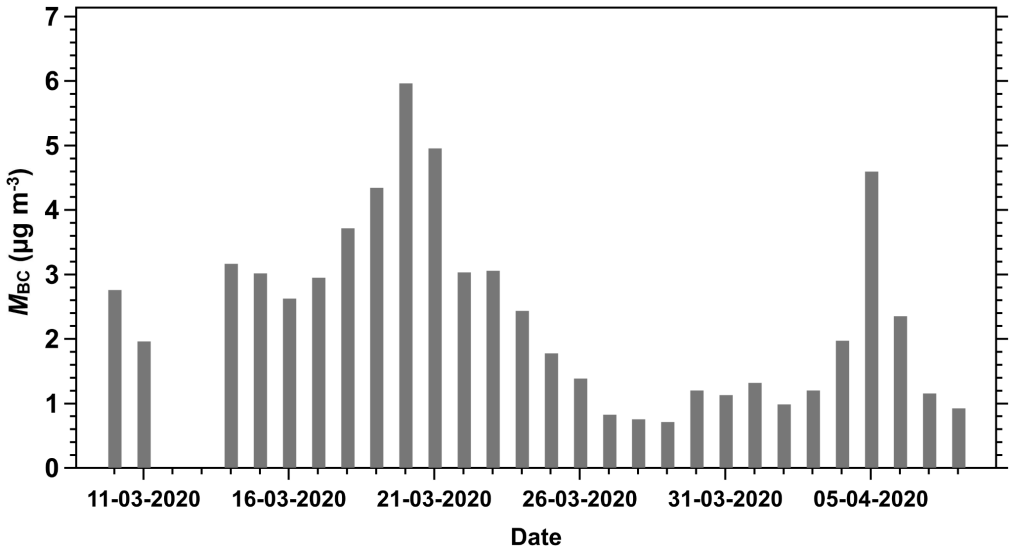

Fig. 11. M_{BC} from March 10, 2020 to April 8, 2020.

4 CONCLUSIONS

Year-round BC measurements were made at an urban site in Delhi using COSMOS. Seasonal and monthly variation of M_{BC} is analyzed to find season- and month-specific causes and sources. Winter and post-monsoon are the most polluted seasons. It is found that meteorological conditions encompass with topography of Delhi play an important role in observed variation. Fire spot and air mass trajectory analyses revealed that in post-monsoon (October and November), the regional transport of pollution due to crop-residual burning in nearby states is important contributing factor for elevation of M_{BC} in Delhi. However, in winter, combined effect of increased local emissions and non-favorable meteorological conditions are responsible for very high M_{BC}. Emission from open burning by local people to keep warm themselves during winters could be the primary reason for increased local emissions. Furthermore, sudden increase in local emissions due to cracker burning on festivals is found to be the responsible factor for very dangerous levels of M_{BC} (1-hour average > 40 μg m^{-3}). COVID-19 lockdown had a positive effect on air quality as M_{BC} decreased up to three times due to traffic and local emission source reduction.

Monthly variation of BC concentrations showed strong correlation with meteorological parameters. Furthermore, BC concentrations were highest during winter season when topography of Delhi and meteorological conditions play a major role. Longer-term measurements will improve our quantitative understanding on the contributions of the factors controlling the observed high M_{BC} (i.e., local sources, biomass burning in nearby states or geographical location/topography of Delhi together with meteorology). As per current analysis, it would be sufficed to point out that geographical location/specific topography together with meteorology is important factor for Delhi high BC concentration.

Proper mitigation steps should be taken to control high level of pollution especially in post-monsoon and winter seasons. These could be control over biomass burning (crop burning) in nearby states during October and November and controlling local emission sources (open burning to fight cold, vehicular emission) in winters. Several initiatives have been taken to control crop residual burning in nearby states. New agricultural machinery like happy seeder (https://www.ideasforindia.in/topics/environment/happy-seeder-a-solution-to-agricultural-fires-in-north-india.html) and super straw management system (Bhattacharyya *et al.*, 2021) are promising innovations which can potentially alleviate the crop-residue burning issue. However, not much focus has been given to control local emission sources in winters. Furthermore, implementation of ban on crackers is required to control emissions during festivals like Diwali and New Year. More rigorous study primarily focused on quantification of local emission source contribution to overall BC pollution (traffic, local open burning in winters and cracker burning) in Delhi is the need of the hour.

Further, to evaluate the representativeness of M_{BC} data, we have compared these data with the Aethalometer data obtained from nearby monitoring stations, and also with satellite data, i.e., Modern-Era Retrospective analysis for Research and Applications - version 2 (MERRA-2)'s surface black carbon data of Delhi. Reasonably good correlations of M_{BC} data with the other data suggest that M_{BC} data reported in this study represent reasonably well the BC variations in Delhi for the study period.

ACKNOWLEDGMENTS

AM is thankful to University Grant Commission (UGC) for providing the fellowship under UGC-SRF scheme (P90802). Authors from CSIR-NPL thank to the Director, CSIR-NPL for providing all support to carry out this work, and further extend their thanks to Heads (present and past) of ESBM, Division #3.0, and students of Gas Metrology group for their help and support. This work was also supported by the Environment Research and Technology Development Fund (JPMEERF20202003) of the Environmental Restoration and Conservation Agency of Japan, and the Japanese Ministry of Education, Culture, Sports, Science, and Technology (MEXT), Japan Society for the Promotion of Science KAKENHI Grants (JP20H00638), and the Arctic Challenge for Sustainability II (ArCS II) project (JPMXD1420318865).

SUPPLEMENTARY MATERIAL

Supplementary material for this article can be found in the online version at https://doi.org/10.4209/aaqr.220128

REFERENCES

Attri, S.D., Tyagi, A. (2010). Climate profile of India. Environ. Meteorol. India Meteorol. Dep. 1–122.

Balakrishnan, K., Dey, S., Gupta, T., Dhaliwal, R.S., Brauer, M., Cohen, A.J., Stanaway, J.D., Beig, G., Joshi, T.K., Aggarwal, A.N., Sabde, Y., Sadhu, H., Frostad, J., Causey, K., Godwin, W., Shukla, D.K., Kumar, G.A., Varghese, C.M., Muraleedharan, P., Agrawal, A., *et al.* (2019). The impact of air pollution on deaths, disease burden, and life expectancy across the states of India: The Global Burden of Disease Study 2017. Lancet Planet. Heath 3, e26–e39. https://doi.org/10.1016/S2542-5196(18)30261-4

Bali, K., Mishra, A.K., Singh, S. (2017). Impact of anomalous forest fire on aerosol radiative forcing and snow cover over Himalayan region. Atmos. Environ. 150, 264–275. https://doi.org/10.1016/j.atmosenv.2016.11.061

Bhattacharyya, P., Bisen, J., Bhaduri, D., Priyadarsini, S., Munda, S., Chakraborti, M., Adak, T., Panneerselvam, P., Mukherjee, A.K., Swain, S.L., Dash, P.K., Padhy, S.R., Nayak, A.K., Pathak, H., Arora, S., Nimbrayan, P. (2021). Turn the wheel from waste to wealth: Economic and environmental gain of sustainable rice straw management practices over field burning in reference to India. Sci. Total Environ. 775, 145896. https://doi.org/10.1016/j.scitotenv.2021.145896

Bikkina, S., Andersson, A., Kirillova, E.N., Holmstrand, H., Tiwari, S., Srivastava, A.K., Bisht, D.S., Gustafsson, Ö. (2019). Air quality in megacity Delhi affected by countryside biomass burning. Nat. Sustain. 2, 200–205. https://doi.org/10.1038/s41893-019-0219-0

Bisht, D.S., Dumka, U.C., Kaskaoutis, D.G., Pipal, A.S., Srivastava, A.K., Soni, V.K., Attri, S.D., Sateesh, M., Tiwari, S. (2015). Carbonaceous aerosols and pollutants over Delhi urban environment: Temporal evolution, source apportionment and radiative forcing. Sci. Total Environ. 521–522, 431–445. https://doi.org/10.1016/j.scitotenv.2015.03.083

Bond, T.C., Anderson, T.L., Campbell, D. (1999). Calibration and intercomparison of filter-based measurements of visible light absorption by aerosols. Aerosol Sci. Technol. 30, 582–600. https://doi.org/10.1080/027868299304435

Bond, T.C., Bhardwaj, E., Dong, R., Jogani, R., Jung, S., Roden, C., Streets, D.G., Trautmann, N.M.

(2007). Historical emissions of black and organic carbon aerosol from energy-related combustion, 1850-2000. Global Biogeochem. Cycles 21, 1–16. https://doi.org/10.1029/2006GB002840

Bond, T.C., Doherty, S.J., Fahey, D.W., Forster, P.M., Berntsen, T., Deangelo, B.J., Flanner, M.G., Ghan, S., Kärcher, B., Koch, D., Kinne, S., Kondo, Y., Quinn, P.K., Sarofim, M.C., Schultz, M.G., Schulz, M., Venkataraman, C., Zhang, H., Zhang, S., Bellouin, N., *et al.* (2013). Bounding the role of black carbon in the climate system: A scientific assessment. J. Geophys. Res. 118, 5380–5552. https://doi.org/10.1002/jgrd.50171

Bosilovich, M.G., Lucchesi, R., Suarez, M. (2016). MERRA-2: File Specification. GMAO Office Note No. 9 (Version 1.1), 73 pp. https://gmao.gsfc.nasa.gov/pubs/docs/Bosilovich785.pdf

Buchard, V., Da Silva, A.M., Colarco, P.R., Darmenov, A., Randles, C.A., Govindaraju, R., Torres, O., Campbell, J., Spurr, R. (2015). Using the OMI aerosol index and absorption aerosol optical depth to evaluate the NASA MERRA Aerosol Reanalysis. Atmos. Chem. Phys. 15, 5743–5760. https://doi.org/10.5194/acp-15-5743-2015

Chen, Y., Schleicher, N., Fricker, M., Cen, K., Liu, X.L., Kaminski, U., Yu, Y., Wu, X.F., Norra, S. (2016). Long-term variation of black carbon and $PM_{2.5}$ in Beijing, China with respect to meteorological conditions and governmental measures. Environ. Pollut. 212, 269–278. https://doi.org/10.1016/j.envpol.2016.01.008

Crilley, L.R., Bloss, W.J., Yin, J., Beddows, D.C.S., Harrison, R.M., Allan, J.D., Young, D.E., Flynn, M., Williams, P., Zotter, P., Prevot, A.S.H., Heal, M.R., Barlow, J.F., Halios, C.H., Lee, J.D., Szidat, S., Mohr, C. (2015). Sources and contributions of wood smoke during winter in London: Assessing local and regional influences. Atmos. Chem. Phys. 15, 3149–3171. https://doi.org/10.5194/acp-15-3149-2015

Dhaka, S.K., Chetna, Kumar, V., Panwar, V., Dimri, A.P., Singh, N., Patra, P.K., Matsumi, Y., Takigawa, M., Nakayama, T., Yamaji, K., Kajino, M., Misra, P., Hayashida, S. (2020). $PM_{2.5}$ diminution and haze events over Delhi during the COVID-19 lockdown period: An interplay between the baseline pollution and meteorology. Sci. Rep. 10, 1–8. https://doi.org/10.1038/s41598-020-70179-8

Dumka, U.C., Kaskaoutis, D.G., Tiwari, S., Safai, P.D., Attri, S.D., Soni, V.K., Singh, N., Mihalopoulos, N. (2018). Assessment of biomass burning and fossil fuel contribution to black carbon concentrations in Delhi during winter. Atmos. Environ. 194, 93–109. https://doi.org/10.1016/j.atmosenv.2018.09.033

Evangeliou, N., Platt, S.M., Eckhardt, S., Lund Myhre, C., Laj, P., Alados-Arboledas, L., Backman, J., Brem, B.T., Fiebig, M., Flentje, H., Marinoni, A., Pandolfi, M., Yus-Dìez, J., Prats, N., Putaud, J.P., Sellegri, K., Sorribas, M., Eleftheriadis, K., Vratolis, S., Wiedensohler, A., *et al.* (2021). Changes in black carbon emissions over Europe due to COVID-19 lockdowns. Atmos. Chem. Phys. 21, 2675–2692. https://doi.org/10.5194/acp-21-2675-2021

Friedlingstein, P., Jones, M.W., O'Sullivan, M., Andrew, R.M., Hauck, J., Peters, G.P., Peters, W., Pongratz, J., Sitch, S., Le Quéré, C., Bakker, D.C.E., Canadell, J.G., Ciais, P., Jackson, R.B., Anthoni, P., Barbero, L., Bastos, A., Bastrikov, V., Becker, M., Bopp, L., *et al.* (2019). Global Carbon Budget 2019. Earth Syst. Sci. Data 11, 1783–1838. https://doi.org/10.5194/essd-11-1783-2019

Ghei, D., Sane, R. (2018). Estimates of air pollution in Delhi from the burning of firecrackers during the festival of Diwali. PLoS One 13, 1–11. https://doi.org/10.1371/journal.pone.0200371

Gogoi, M.M., Suresh Babu, S., Krishna Moorthy, K., Manoj, M.R., Chaubey, J.P. (2013). Absorption characteristics of aerosols over the northwestern region of India: Distinct seasonal signatures of biomass burning aerosols and mineral dust. Atmos. Environ. 73, 92–102. https://doi.org/10.1016/j.atmosenv.2013.03.009

Hansen, A.D.A. (2005). The Aethalometer - User Manual, ver. 2005.07 Magee Scientific Company, Berkeley, California, US.

Healy, R.M., Sofowote, U., Su, Y., Debosz, J., Noble, M., Jeong, C.H., Wang, J.M., Hilker, N., Evans, G.J., Doerksen, G., Jones, K., Munoz, A. (2017). Ambient measurements and source apportionment of fossil fuel and biomass burning black carbon in Ontario. Atmos. Environ. 161, 34–47. https://doi.org/10.1016/j.atmosenv.2017.04.034

Henry, R., Norris, G.A., Vedantham, R., Turner, J.R. (2009). Source region identification using kernel smoothing. Environ. Sci. Technol. 43, 4090–4097. https://doi.org/10.1021/es8011723

Hyvärinen, A.P., Lihavainen, H., Komppula, M., Panwar, T.S., Sharma, V.P., Hooda, R.K., Viisanen, Y. (2010). Aerosol measurements at the Gual Pahari EUCAARI station: Preliminary results from

in-situ measurements. Atmos. Chem. Phys. 10, 7241–7252. https://doi.org/10.5194/acp-10-7241-2010

IQAir (2019). World Air Quality. 2019 World Air Quality Report 1–22.

IQAir (2020). 2020 World Air Quality Report: Region & City $PM_{2.5}$ Ranking. IQAir 1–41.

Irwin, M., Kondo, Y., Moteki, N. (2015). An empirical correction factor for filter-based photo-absorption black carbon measurements. J. Aerosol Sci. 80, 86–97. https://doi.org/10.1016/j.jaerosci.2014.11.001

Janssen, N.A.H., Hoek, G., Simic-Lawson, M., Fischer, P., van Bree, L., Brink, H. Ten, Keuken, M., Atkinson, R.W., Ross Anderson, H., Brunekreef, B., Cassee, F.R. (2011). Black carbon as an additional indicator of the adverse health effects of airborne particles compared with PM_{10} and $PM_{2.5}$. Environ. Health Perspect. 119, 1691–1699. https://doi.org/10.1289/ehp.1003369

Jose, S., Gharai, B., Rao, P.V.N. (2017). Cross-sectional view of atmospheric aerosols over an urban location in Central India. Aerosol Air Qual. Res. 17, 761–775. https://doi.org/10.4209/aaqr.2016.04.0154

Klimont, Z., Kupiainen, K., Heyes, C., Purohit, P., Cofala, J., Rafaj, P., Borken-Kleefeld, J., Schöpp, W. (2017). Global anthropogenic emissions of particulate matter including black carbon. Atmos. Chem. Phys. 17, 8681–8723. https://doi.org/10.5194/acp-17-8681-2017

Kondo, Y., Sahu, L., Kuwata, M., Miyazaki, Y., Takegawa, N., Moteki, N., Imaru, J., Han, S., Nakayama, T., Oanh, N.T.K., Hu, M., Kim, Y.J., Kita, K. (2009). Stabilization of the mass absorption cross section of black carbon for filter-based absorption photometry by the use of a heated inlet. Aerosol Sci. Technol. 43, 741–756. https://doi.org/10.1080/02786820902889879

Kondo, Y., Sahu, L., Moteki, N., Khan, F., Takegawa, N., Liu, X., Koike, M., Miyakawa, T. (2011). Consistency and traceability of black carbon measurements made by laser-induced incandescence, thermal-optical transmittance, and filter-based photo-absorption techniques. Aerosol Sci. Technol. 45, 295–312. https://doi.org/10.1080/02786826.2010.533215

Kulkarni, S.H., Ghude, S.D., Jena, C., Karumuri, R.K., Sinha, B., Sinha, V., Kumar, R., Soni, V.K., Khare, M. (2020). How much does large-scale crop residue burning affect the air quality in Delhi? Environ. Sci. Technol. 54, 4790–4799. https://doi.org/10.1021/acs.est.0c00329

Kumar, R.R., Soni, V.K., Jain, M.K. (2020). Evaluation of spatial and temporal heterogeneity of black carbon aerosol mass concentration over India using three year measurements from IMD BC observation network. Sci. Total Environ. 723, 138060. https://doi.org/10.1016/j.scitotenv.2020.138060

Kumar, S., Aggarwal, S.G., Malherbe, J., Barre, J.P.G., Berail, S., Gupta, P.K., Donard, O.F.X. (2016). Tracing dust transport from Middle-East over Delhi in March 2012 using metal and lead isotope composition. Atmos. Environ. 132, 179–187. https://doi.org/10.1016/j.atmosenv.2016.03.002

Kumar, S., Aggarwal, S.G., Sarangi, B., Malherbe, J., Barre, J.P.G., Berail, S., Séby, F., Donard, O.F.X. (2018). Understanding the influence of open-waste burning on urban aerosols using metal tracers and lead isotopic composition. Aerosol Air Qual. Res. 18, 2433–2446. https://doi.org/10.4209/aaqr.2017.11.0510

Kuo, C.L. (2017). Assessments of Ali, Dome A, and Summit Camp for mm-wave observations using MERRA-2 reanalysis. Astrophys. J. 848, 64. https://doi.org/10.3847/1538-4357/aa8b74

Liu, Q., Ma, T., Olson, M.R., Liu, Y., Zhang, T., Wu, Y., Schauer, J.J. (2016). Temporal variations of black carbon during haze and non-haze days in Beijing. Sci. Rep. 6, 1–10. https://doi.org/10.1038/srep33331

Liu, T., Marlier, M.E., DeFries, R.S., Westervelt, D.M., Xia, K.R., Fiore, A.M., Mickley, L.J., Cusworth, D.H., Milly, G. (2018). Seasonal impact of regional outdoor biomass burning on air pollution in three Indian cities: Delhi, Bengaluru, and Pune. Atmos. Environ. 172, 83–92. https://doi.org/10.1016/j.atmosenv.2017.10.024

Mahato, S., Pal, S., Ghosh, K.G. (2020). Effect of lockdown amid COVID-19 pandemic on air quality of the megacity Delhi, India. Sci. Total Environ. 730, 139086. https://doi.org/10.1016/j.scitotenv.2020.139086

Malik, A., Aggarwal, S.G. (2021). A review on the techniques used and status of equivalent black carbon measurement in two major Asian countries. Asian J. Atmos. Environ. 15, 1–32. https://doi.org/10.5572/AJAE.2021.044

Miyakawa, T., Oshima, N., Taketani, F., Komazaki, Y., Yoshino, A., Takami, A., Kondo, Y., Kanaya, Y. (2017). Alteration of the size distributions and mixing states of black carbon through

transport in the boundary layer in east Asia. Atmos. Chem. Phys. 17, 5851–5864. https://doi.org/10.5194/acp-17-5851-2017

Miyazaki, Y., Kondo, Y., Sahu, L.K., Imaru, J., Fukushima, N., Kano, M. (2008). Performance of a newly designed continuous soot monitoring system (COSMOS). J. Environ. Monit. 10, 1195–1201. https://doi.org/10.1039/b806957c

Mori, T., Ohata, S., Morino, Y., Koike, M., Moteki, N., Kondo, Y. (2020). Changes in black carbon and $PM_{2.5}$ in Tokyo in 2003–2017. Proc. Jpn. Acad., Ser. B 96, 122–129. https://doi.org/10.2183/pjab.96.010

Moteki, N., Kondo, Y. (2010). Dependence of laser-induced incandescence on physical properties of black carbon aerosols: Measurements and theoretical interpretation. Aerosol Sci. Technol. 44, 663–675. https://doi.org/10.1080/02786826.2010.484450

Mousavi, A., Sowlat, M.H., Hasheminassab, S., Polidori, A., Sioutas, C. (2018). Spatio-temporal trends and source apportionment of fossil fuel and biomass burning black carbon (BC) in the Los Angeles Basin. Sci. Total Environ. 640–641, 1231–1240. https://doi.org/10.1016/j.scitotenv.2018.06.022

Mukherjee, T., Asutosh, A., Pandey, S.K., Yang, L., Gogoi, P.P., Panwar, A., Vinoj, V. (2018). Increasing potential for air pollution over megacity New Delhi: A study based on 2016 diwali episode. Aerosol Air Qual. Res. 18, 2510–2518. https://doi.org/10.4209/aaqr.2017.11.0440

Navinya, C.D., Vinoj, V., Pandey, S.K. (2020). Evaluation of $PM_{2.5}$ surface concentrations simulated by NASA's MERRA Version 2 aerosol reanalysis over india and its relation to the air quality index. Aerosol Air Qual. Res. 20, 1329–1339. https://doi.org/10.4209/aaqr.2019.12.0615

Ogren, J.A. (2010). Comment on "calibration and intercomparison of filter-based measurements of visible light absorption by aerosols." Aerosol Sci. Technol. 44, 589–591. https://doi.org/10.1080/02786826.2010.482111

Ohata, S., Kondo, Y., Moteki, N., Mori, T., Yoshida, A., Sinha, P.R., Koike, M. (2019). Accuracy of black carbon measurements by a filter-based absorption photometer with a heated inlet. Aerosol Sci. Technol. 53, 1079–1091. https://doi.org/10.1080/02786826.2019.1627283

Ohata, S., Mori, T., Kondo, Y., Sharma, S., Hyvärinen, A., Andrews, E., Tunved, P., Asmi, E., Backman, J., Servomaa, H., Veber, D., Eleftheriadis, K., Vratolis, S., Krejci, R., Zieger, P., Koike, M., Kanaya, Y., Yoshida, A., Moteki, N., Zhao, Y., *et al.* (2021). Estimates of mass absorption cross sections of black carbon for filter-based absorption photometers in the Arctic. Atmos. Meas. Tech. 14, 6723–6748. https://doi.org/10.5194/amt-14-6723-2021

Paliwal, U., Sharma, M., Burkhart, J.F. (2016). Monthly and spatially resolved black carbon emission inventory of India: Uncertainty analysis. Atmos. Chem. Phys. 16, 12457–12476. https://doi.org/10.5194/acp-16-12457-2016

Petit, J.E., Favez, O., Albinet, A., Canonaco, F. (2017). A user-friendly tool for comprehensive evaluation of the geographical origins of atmospheric pollution: Wind and trajectory analyses. Environ. Model. Softw. 88, 183–187. https://doi.org/10.1016/j.envsoft.2016.11.022

Qin, W., Zhang, Y., Chen, J., Yu, Q., Cheng, S., Li, W., Liu, X., Tian, H. (2019). Variation, sources and historical trend of black carbon in Beijing, China based on ground observation and MERRA-2 reanalysis data. Environ. Pollut. 245, 853–863. https://doi.org/10.1016/j.envpol.2018.11.063

Rajak, R., Chattopadhyay, A. (2020). Short and Long Term Exposure to Ambient Air Pollution and Impact on Health in India: A Systematic Review. Int. J. Environ. Health Res. 30, 593–617. https://doi.org/10.1080/09603123.2019.1612042

Rana, A., Jia, S., Sarkar, S. (2019). Black carbon aerosol in India: A comprehensive review of current status and future prospects. Atmos. Res. 218, 207–230. https://doi.org/10.1016/j.atmosres.2018.12.002

Rao, P.S., Gajghate, D.G., Gavane, A.G., Suryawanshi, P., Chauhan, C., Mishra, S., Gupta, N., Rao, C.V.C., Wate, S.R. (2012). Air quality status during diwali festival of India: A case study. Bull. Environ. Contam. Toxicol. 89, 376–379. https://doi.org/10.1007/s00128-012-0669-9

Saha, A., Despiau, S. (2009). Seasonal and diurnal variations of black carbon aerosols over a Mediterranean coastal zone. Atmos. Res. 92, 27–41. https://doi.org/10.1016/j.atmosres.2008.07.007

Sahu, L.K., Kondo, Y., Miyazaki, Y., Pongkiatkul, P., Kim Oanh, N.T. (2011). Seasonal and diurnal variations of black carbon and organic carbon aerosols in Bangkok. J. Geophys. Res. 116, D15302. https://doi.org/10.1029/2010JD015563

Sateesh, M., Soni, V.K., Raju, P.V.S. (2018). Effect of diwali firecrackers on air quality and aerosol optical properties over mega city (Delhi) in India. Earth Syst. Environ. 2, 293–304. https://doi.org/10.1007/s41748-018-0054-x

Sedlacek, A.J. (2016). Aethalometer™ Instrument Handbook. U.S. Dep. Energy DOE/SC-ARM, 1–28.

Sharma, D., Srivastava, A.K., Ram, K., Singh, A., Singh, D. (2017). Temporal variability in aerosol characteristics and its radiative properties over Patiala, northwestern part of India: Impact of agricultural biomass burning emissions. Environ. Pollut. 231, 1030–1041. https://doi.org/10.1016/j.envpol.2017.08.052

Singh, A.K., Srivastava, A. (2020). The impact of fireworks emissions on air quality in Delhi, India. Environ. Claims J. 32, 289–309. https://doi.org/10.1080/10406026.2020.1756078

Sitnov, S.A., Mokhov, I.I., Likhosherstova, A.A. (2020). Exploring large-scale black-carbon air pollution over Northern Eurasia in summer 2016 using MERRA-2 reanalysis data. Atmos. Res. 235, 104763. https://doi.org/10.1016/j.atmosres.2019.104763

Srivastava, A.K., Bisht, D.S., Ram, K., Tiwari, S., Srivastava, M.K. (2014). Characterization of carbonaceous aerosols over Delhi in Ganga basin: Seasonal variability and possible sources. Environ. Sci. Pollut. Res. 21, 8610–8619. https://doi.org/10.1007/s11356-014-2660-y

Surendran, D.E., Beig, G., Ghude, S.D., Panicker, A.S., Manoj, M.G., Chate, D.M., Ali, K. (2013). Radiative forcing of black carbon over Delhi. Int. J. Photoenergy 2013, 313652. https://doi.org/10.1155/2013/313652

Talukdar, S., Jana, S., Maitra, A., Gogoi, M.M. (2015). Characteristics of black carbon concentration at a metropolitan city located near land-ocean boundary in Eastern India. Atmos. Res. 153, 526–534. https://doi.org/10.1016/j.atmosres.2014.10.014

Tiwari, S., Srivastava, A.K., Bisht, D.S., Parmita, P., Srivastava, M.K., Attri, S.D. (2013). Diurnal and seasonal variations of black carbon and $PM_{2.5}$ over New Delhi, India: Influence of meteorology. Atmos. Res. 125–126, 50–62. https://doi.org/10.1016/j.atmosres.2013.01.011

Tiwari, S., Bisht, D.S., Srivastava, A.K., Pipal, A.S., Taneja, A., Srivastava, M.K., Attri, S.D. (2014). Variability in atmospheric particulates and meteorological effects on their mass concentrations over Delhi, India. Atmos. Res. 145–146, 45–56. https://doi.org/10.1016/j.atmosres.2014.03.027

Tyagi, C., Gupta, N.C., Soni, V.K., Sarma, K. (2020). Seasonal variation of black carbon emissions in urban Delhi, India. Environ. Claims J. 32, 101–111. https://doi.org/10.1080/10406026.2019.1699723

Wang, R., Tao, S., Wang, W., Liu, J., Shen, H., Shen, G., Wang, B., Liu, X., Li, W., Huang, Y., Zhang, Y., Lu, Y., Chen, H., Chen, Y., Wang, C., Zhu, D., Wang, X., Li, B., Liu, W., Ma, J. (2012). Black carbon emissions in China from 1949 to 2050. Environ. Sci. Technol. 46, 7595–7603. https://doi.org/10.1021/es3003684

Wu, Y., Zhang, R., Tian, P., Tao, J., Hsu, S.C., Yan, P., Wang, Q., Cao, J., Zhang, X., Xia, X. (2016). Effect of ambient humidity on the light absorption amplification of black carbon in Beijing during January 2013. Atmos. Environ. 124, 217–223. https://doi.org/10.1016/j.atmosenv.2015.04.041

Xu, L., Zhang, J., Sun, X., Xu, S., Shan, M., Yuan, Q., Liu, L., Du, Z., Liu, D., Xu, D., Song, C., Liu, B., Lu, G., Shi, Z., Li, W. (2020a). Variation in concentration and sources of black carbon in a megacity of China during the COVID-19 pandemic. Geophys. Res. Lett. 47, e2020GL090444. https://doi.org/10.1029/2020GL090444

Xu, X., Yang, X., Zhu, B., Tang, Z., Wu, H., Xie, L. (2020b). Characteristics of MERRA-2 black carbon variation in east China during 2000–2016. Atmos. Environ. 222, 117140. https://doi.org/10.1016/j.atmosenv.2019.117140

Zanatta, M., Laj, P., Gysel, M., Baltensperger, U., Vratolis, S., Eleftheriadis, K., Kondo, Y., Dubuisson, P., Winiarek, V., Kazadzis, S., Tunved, P., Jacobi, H.W. (2018). Effects of mixing state on optical and radiative properties of black carbon in the European Arctic. Atmos. Chem. Phys. 18, 14037–14057. https://doi.org/10.5194/acp-18-14037-2018

Zhang, L., Shen, F., Gao, J., Cui, S., Yue, H., Wang, J., Chen, M., Ge, X. (2020). Characteristics and potential sources of black carbon particles in suburban Nanjing, China. Atmos. Pollut. Res. 11, 981–991. https://doi.org/10.1016/j.apr.2020.02.011